Time Series Analysis in Mactaquac Dam using Distributed Temperature Sensing for seasonal seepage reconnaissance

Emanuel de Gante
UNB EE 6563
University of New Brunswick
Fredericton, Canada
emanuel.degante@unb.ca

I – INTRODUCTION

The Mactaquac generating station is a hydroelectric facility located on the Saint John River 20 kilometers upstream of Fredericton and has been operating since 1968. Since the 1980s concrete portions of the hydro station have been affected by a chemical alkali-aggregate reaction causing the concrete to swell and crack-requiring substantial annual maintenance and repairs. NB Power is proposing a project to ensure the station can operate to its intended 100-year lifespan with a modified approach to maintenance [1].

All dams are designed and constructed to allow some seepage from the headpond to the downstream toe. Seepage becomes a concern when it leads to internal erosion, where statistical analyses [2] indicate that about 50% of embankment dam failures in the world before 1999 were due to internal erosion. The location of the internal erosion may occur within the embankment, in the foundation or from the embankment into the foundation.

Seepage is the infiltration of water from the upstream reservoir of the dam towards the downstream face. Water flow in porous media is governed y the hydraulic conductivity of the material and the hydraulic head gradient. Heat is transported through porous media primarily by conduction and convection, with convection being enhanced in regions with concentrated seepage flow. Thus, heat can be used as a tracer and temperature analysis can be used as a method for seepage detection and monitoring [3]. Temperature monitoring can detect anomalous temperature variations triggered by increased seepage flow [4]. Fibre Optic Distributed Temperature Systems have been installed in embankment around the world to monitor temperature and detect leaks or concentrated seepage along the embankment.

There are two main methods to use fibre optics DTS for seepage recognition, the passive method and the active method. The passive method requires several months or years to adequately capture the seasonal temperature where reservoir water temperature oscillations do not propagate deep into the dam, and the temperature fluctuations within the dam should be relatively stable especially at distances far from the reservoir however when anomalous seepage occurs, temperature anomalies will be transported into the dam structure by means of convection and the normal temperature will be distorted. The magnitude and velocity of seepage flow may be estimated by means of the time lag and intensity of the temperature anomaly observing seasonal temperature variations [5][6]. The active method requires a

heating source where the Fibre Optic detects the dissipated heat in much shorter periods of time compared to the passive method, not capturing seasonal components or other environmental

fluctuations that have a more direct impact in the seepage through the seasons.

There is fibre optic DTS system installed at Mactaquac in the south end pier in vertical position and it is configured to record temperature through the fibre optic string every 30 minutes. The data is recorded in .ddf extension containing date and time of the measurement event, temperature measurement every 0.5 ft along the total length of the cable, stokes and anti stokes from Raman spectroscopy to calculate temperature. Data is processed into h5 format for data management purposes and into hourly, daily and weekly average time lapses. A second data process step converts the data set into a csv file containing the time stamp (weekly, daily, or hourly averages) and temperature for each of the 285 equivalent pseudo nodes allocated through the elevation of the head pond. There is a total of 8 years of temperature measurements with intervals in 2017 and 2018 where temperature was not recorded because the Fibre Optic was pulled out for major maintenance procedures within the embankment.

Figure (1) Mactaquac Dam and location of the Fibre Optic DTS installed in the embankment.

There is an anomalous temperature behavior occurring during the colder periods located between an elevation of 118’ and 128’. This heat pulses are inferred to be seepage moving through the embankment taking weeks to move from the headpond wall to the frontal wall of the dam just as the passive method suggest.

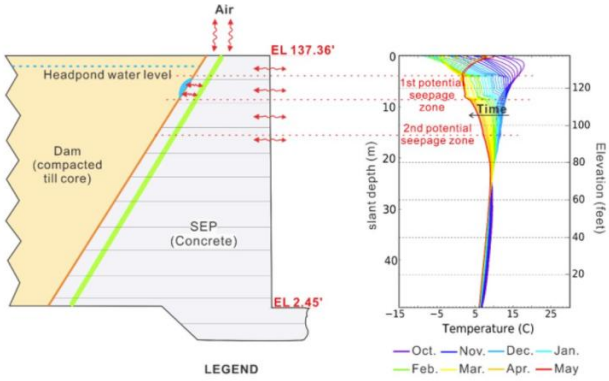

Figure (2) Schematics of the Fibre Optic DTS installation at Mactaquac and Elevation vs Temperature profiles.

The following elevation vs temperature profiles show how temperature differs at a specific elevation in different seasons, proving that the temperature anomaly is seasonal.

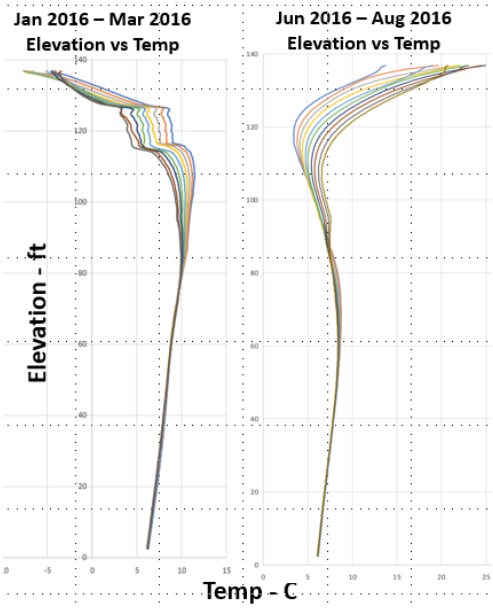

Figure 3) Fibre Optic DTS Temperature vs elevation profile for cold and warm seasons.

There is an equivalent of 24 pseudo nodes comprehending the elevation located between 118’ and 128’, this can be described as a

multivariate time series approach where each component represents a specific elevation point and anomalies can be analysed by the behavior of the relation between each other or individually.

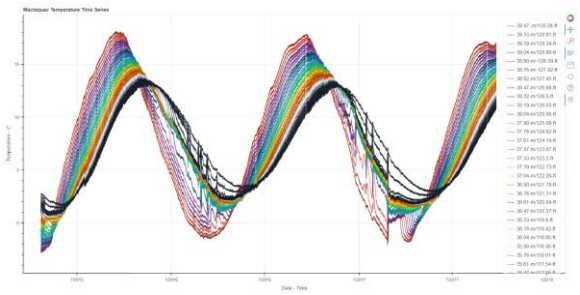

Figure 4) Temperature Time Series of 24 pseudo nodes located at an elevation between 128' and 118'.

Figure 5) ○ Fibre Optic DTS data in the till core of the embankment dam ○ 10 – Thermistor string located in the headpond adjacent to the SEP.

There is a Thermistor string temporarily installed in the adjacent wall of the headpond next to the sluiceway. This string operated from Jun 6th, 2021, to September 11th, 2021, at 124 ft, 118.06 ft, 111.9 ft, 104.19 ft, 82.62 ft, 67.2 ft, 51.05 ft, 34.63 ft, and 18.24 ft. This thermistor string is capable of detecting temperature changes occurring in the subsurface caused by the operation of the walls in the sluiceway.

In this paper ARIMA and PCA will be used to detect temperature anomalies (out of the pattern) in the time series. Also, Multivariate Dynamic Time Warping will be used for template matching to locate repeated anomalies in time, and Granger Causality test will be used with the thermistor data set to see if the data can be used to forecast DTS data.

2. LITERATURE REVIEW

Zheng et al [7] propose an interesting approach based on ARIMA based real time monitoring and warning algorithm for anomaly detection where he uses a Fiber Mechanical & Thermal multiparameter Instrument where they forecast their thermal measurements based on their raw data and perform several sensitivity analyses to calculate a threshold based on the number of truly detected abnormities and the number of wrongly detected abnormities. Similar to Zhang, Pena et al. [8] propose a similar method to use ARIMA to detect anomalies using forecasting methods for IP networks behavior by analyzing the forecast behavior used in the detection of volume anomalies. The most interesting approach is the one proposed by Yaaakob et al [9] where it is proposed to use ARIMA to measure error in internet traffic flow by forecasting a new time series based on the internet traffic flow, calculating the error between them and stablishing a threshold to detect major anomalies within the signal. Tron et al [12] use ARIMA anomaly detection on patients with schizophrenia disorders to monitor patient motor activity in a close ward hospital.

Principal component analysis is used for dimensionality reduction in classification problems, but it can be used to detect anomalies in time series problems too. Jin et al [10] propose the use of PCA to detect abnormal or malicious behavior for data traffic management to avoid confidential information leakage (high frequency data, IP address, accessing trials, query time, operation contents, etc.). This is by decomposing the PCA matrix into M=L+S, where M is the observation matrix, L is the matrix having low rank and S is a sparse matrix having a few nonzero elements (similar to SVD). By arranging each query time series of each user as the matrix M, and reconstructing the matrix M with most

significant variations from the PCA analysis and stablishing threshold to detect outlier. Malioutov[11] describes a mathematical formulation where PCA with conditional value at risk as error metric can drive a low rank approximation.

Gaoming et al [13] use a Dynamic Time Warp approach for template analysis, this is univariate time series for cryptographic chips. They report 80 percent of template match in the four experiments performed. Liang et al [14] Describe how to cluster multivariate time series from large sensors in electronic applications, using K-means to detect underlying patters. Phan et al [15] describe a method for imputation in uncorrelated multivariate time series. By this they us KNN as an imputation technique to fill the gabs and perform the template matching of multivariate time series.

Granger causality is used by Bhattacharjee et al. [16] to infer spatial dependency of meteorological attributes for multivariate analysis. Chvosteková [17] as well as Yonghua [18] perform several analyses to measure the efficiency of Granger causality test to measure the causation to forecast one variable to another.

3. MEDHODS

Data for this project consist of three data sets: The first data set is a continuous distributed temperature measurement of the fibre optic installed in a 50-metre borehole drilled into the concrete structure within 0.5 m of the interface. A 10-thermistor string was installed adjacent to the south end pier next to the sluiceway recording temperature data at different elevations in the headpond, and air temperature obtained from the Fredericton CDA CS measuring station.

A data set for DTS from April 22nd 2015 to September 20th 2017 with an hourly sampling rate will be used for the ARIMA and PCA and Multivariate Time Warping analyses.

Granger causality and multicoinegration will be analyzed with DTS, the thermistor string and Air data at an hourly sampling rate from Jun -11th 2021 to August 7th 2021.

There are some missing data in the thermistor string and the air temperature data, but this will be handled with linear interpolation.

The relative entropy or Kullback-Liebler divergence as a statistical distance measure how the probability distribution Q is different from a second, reference probability distribution P. $D_{KL}(P\ II\ Q)$

The divergence analysis will measure divergence from consecutive temperature distributions in the same period of time in independent elevations or pseudo-nodes will be compared in a consecutive way, and that will locate where are the elevations with larger divergence, locating anomalous zones.

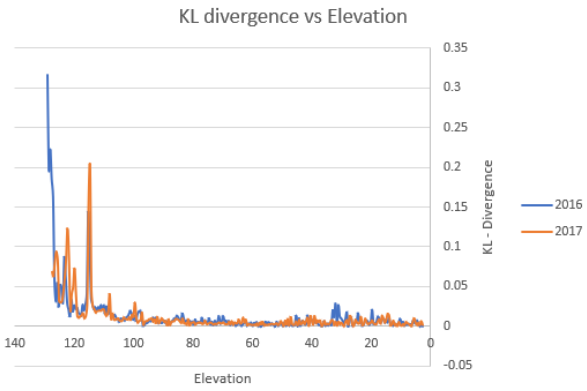

Figure 6) Kullback Lieber divergence for 2016 and 2017. Major divergences occur at an elevation of 128 ft and 118 ft.

The divergence analysis, as well as a temperature gradient analysis, shows that the major divergences occur at a elevation of 128' and 118' making this zone our main target of analysis for this paper.

3.1 ARIMA FOR UNIVARIATE ANOMALY DETECTION

Autoregressive, Integrated Moving Average models for univariate time series analysis allows to forecast the same signal based on previous values. The signal must be stationary and to achieve this the signal has to be differentiated.

The Autoregressive model is based on the idea that the predicted value can be explained as a function of past values.

$$x_t = c + \emptyset_1 x_{t-1} + \emptyset_2 x_{t-2} + \cdots \emptyset_p x_{p-1} + \varepsilon_t$$

, the order of the model is defined by how many points back it looks

Moving Averages.

$$x_t = \varepsilon_t + \theta_1 \varepsilon_{t-1} + \theta_2 \varepsilon_{t-2} + \cdots \theta_p \varepsilon_{t-q}$$

For the model, a daily temperature sample between 22nd April 2015 and 24th September 2017

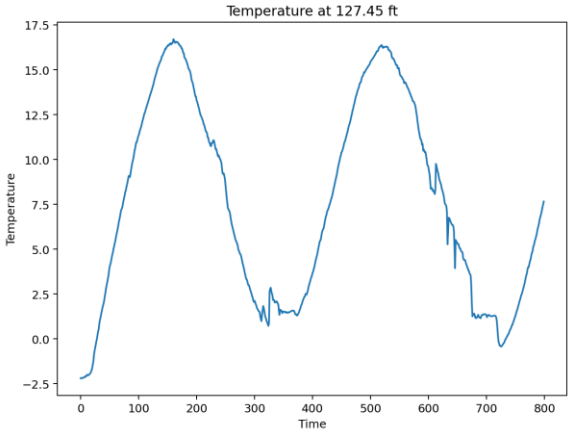

Figure 7) Temperature Time Series at an elevation of 127.45 ft for the period between April 2015 and September 2017.

After performing Augmented Dickey Fuller Test we see that the p-value for this series is 0.14, and it has to be differenced 2 times to get a p-value=0.0000 to achieve stationarity. With this it is confirmed that the series achieved stationarity and the p,q,d order can be selected from autocorrelation and partial autocorrelation functions.

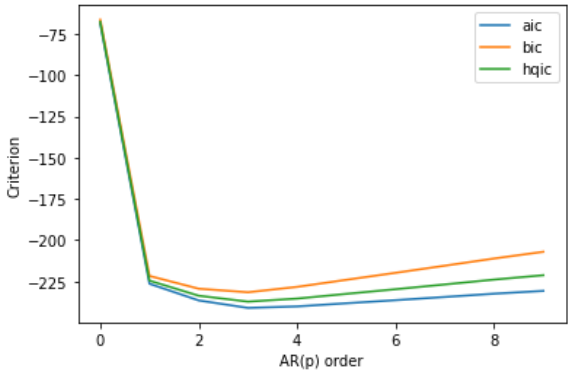

Figure 8) Criterion for AR order p

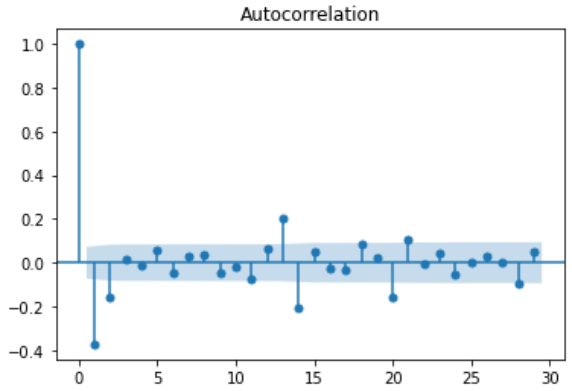

Figure 9) Autocorrelation function of DTS time series at 127.45 ft.

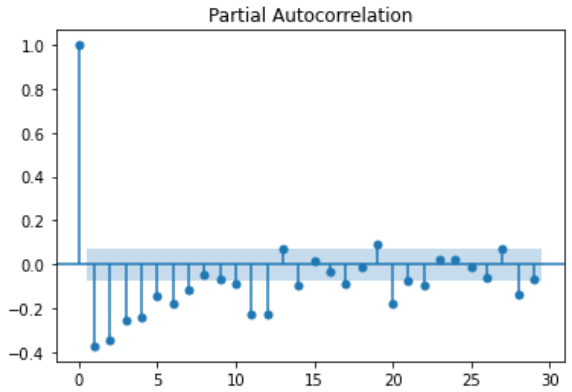

Figure 10) Partial Autocorrelation function of DTS time series at 127.45 ft.

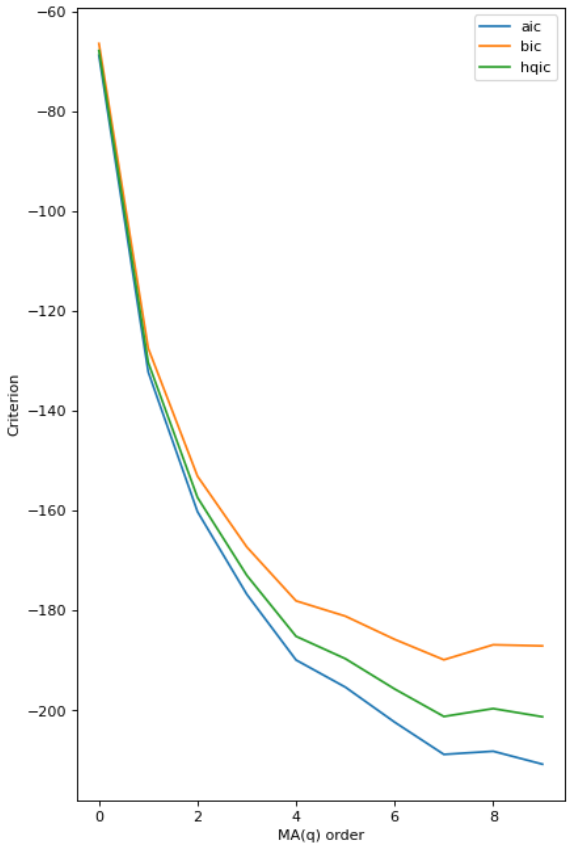

Figure 8) Criterion for MA order q.

Our model selection for our first ARIMA model at an elevation of 127.25 ft is 3,2,2. This procedure will be repeated for selected pseudo nodes to detect their ARIMA model. A 95% confidence interval from their prediction will be used to detect outliers. The forecast error is the difference of the real value minus the predicted value, depending on the magnitude of the error, It will give an estimate of the magnitude of the anomaly of the temperature and when it time happens for each variable.

3.2 PRINCIPAL COMPONENT ANALYSIS

Principal Component Analysis or PCA for Time Series Anomaly Detection can be used to detect outliers in multivariate time series. The DTS temperature time series consist of 24-time independent time series behaving in a sinusoidal pattern. Each time series has a different anomaly magnitude representing a specific elevation in a specific time, but this are related because the anomaly has a higher magnitude in specific zones. Data is arranged in time series format and 70 percent of the series is selected to train the algorithm and 30 percent is selected to test it. After applying the algorithm, the series consist of 24 variables and the series are decomposed into the number of principal components that contain most of the features represented in the series overall.

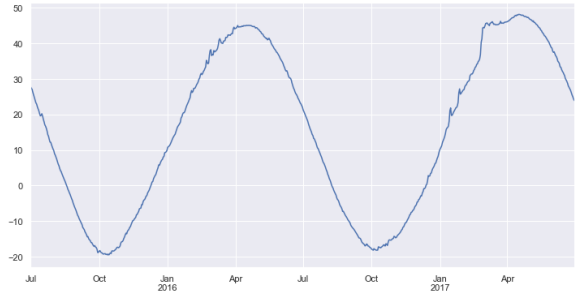

Figure 9: 1 Principal component of the 23 series containing most of the representative features of the series.

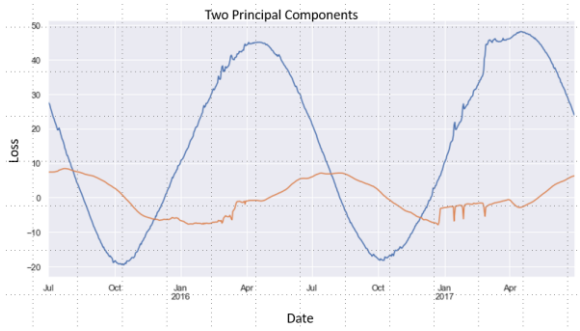

Figure 10: 2 Principal component of the 23 series containing most of the representative features of the series.

Once having the number of principal components, the series can be reconstructed based on the number of principal components, having most of the characteristic features with the combination of the principal components.

Data is arranged in time series format and after performing PCA over the time series, the number of principal components are selected to reconstruct the whole series. An error function comparing the original series vs the reconstructed series will be calculated to point

out a threshold where outliers should be marked.

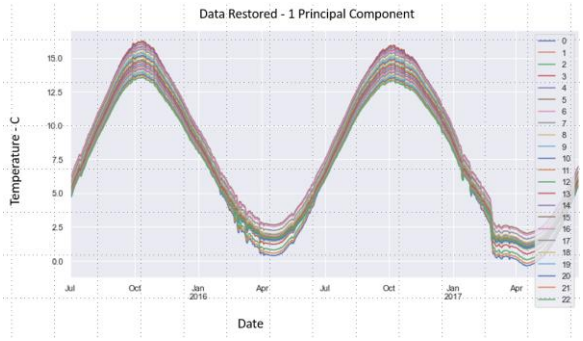

Figure 11: Multivariate Time Series reconstructed with one principal component.

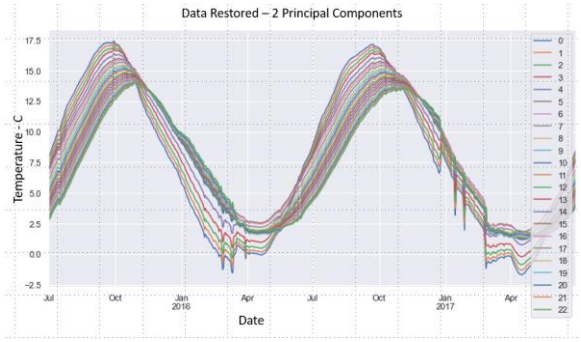

Figure 12: Multivariate Time Series reconstructed with two principal components.

Once reconstructed the series, a loss calculated as the square difference of the original series minus the reconstructed series will give a

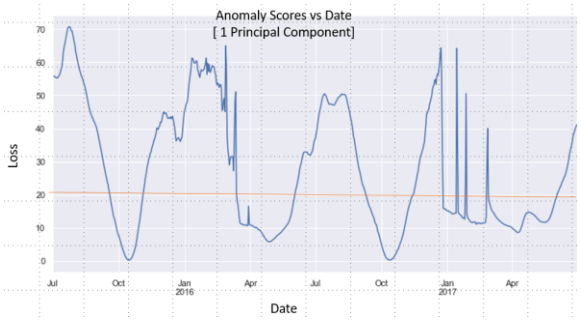

Figure 13: Loss calculated from the square difference of the original series minus the reconstructed series with one principal component.

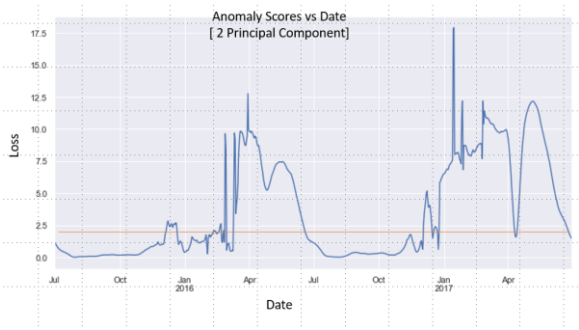

Figure 14: Loss calculated from the square difference of the original series minus the reconstructed series with two principal components.

Once stablished a loss threshold based on the loss of the reconstructed series, those points in time located above the threshold can be accounted as anomalous temperature readings in the series.

3.3 MULTIVARIATE TIME WARPING

Inputs

$x_{1:n}$ and $y_{1:n}$

Cost Matrix $D \in \mathbb{R}^{N+1\ x\ M+1}$

For $i = 1$ to N: $D_{i,0} = \infty$

For $j = 1$ to M: $D_{0,j} = \infty$

$$D_{i,j} = d(x_i, y_i) + \min \begin{pmatrix} D_{i-1,j-1} & (match) \\ D_{i-1,j} & (insertion \\ D_{i,j-1} & (deletion) \end{pmatrix}$$

For multivariate analysis the cosine distance between vectors is used to calculate the cost of alignment.

For multivariate template matching two main temperature anomalies described in the data set were allocated. The first one is represented as a thermal bag occurring the first time between the February the 25th of 2016 to February the 29th of 2016. This event repeat itself in the series 7 times.

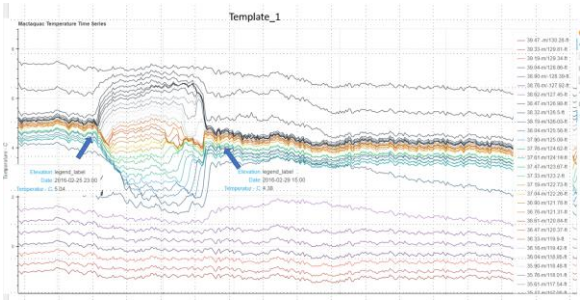

Figure 15: Thermal bag located between February 25th 2016 and February 27th 2016.

Other thermal anomaly is a heat pulse traveling diagonally occurring between November 17th 2016 and December 24th 2016. This event repeats itself three times in the same time lapse.

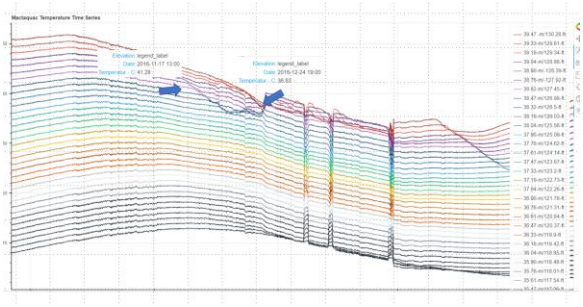

Figure 16: Heat pulse traveling diagonally between November 17th 2016 and December 24th 2016.

A rolling window of 0.05 times the template was calibrated

A rolling window of 0.05 times was calibrated to perform the template dynamic time warping so with this it will be possible to detect

Multivariate dynamic time warping for subsequence detection, where anomalies detected in the 20 timeseries represent head bags and heat pulses will be to find a sequence within a larger sequence (the whole time series) with cosine distance between vectors

A sliding window size 0f 0.05 the length of the anomaly sample will gibe an interpretable alignment cost to detect how many times the template may repeat in the

3.4 GRANGER CAUSALITY

Granger causality will be used to determine if one time series will be used to forecast another.

If the P value is significant $p<0.05$ then the null hypothesis must be rejected determining that the time series is indeed useful. This may not be truly causal, but the variables at least provide predictive information.

The thermistors are located at an elevation of 124.5 ft, 118.06 ft, 111.9 ft, 104.19 ft, 82.61 ft, 51.05 ft, 34.64 ft, 18.24 ft. Granger causality test will be performed to see

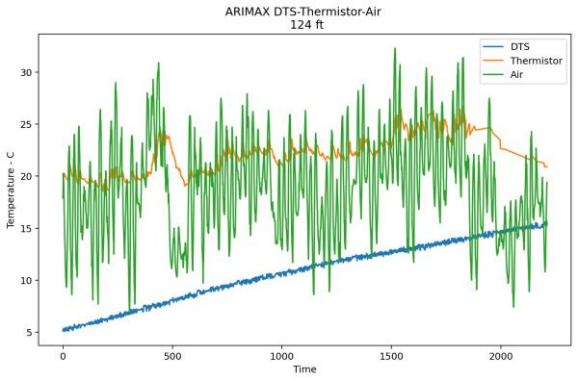

Figure 17) DTS temperature in blue 124.62ft Air Temperature in Green and Thermistor temperature in orange 124.5 ft.

4. RESULTS

The following results were obtained from the different algorithms applied for time series analyses.

4.1 ARIMA RESULTS

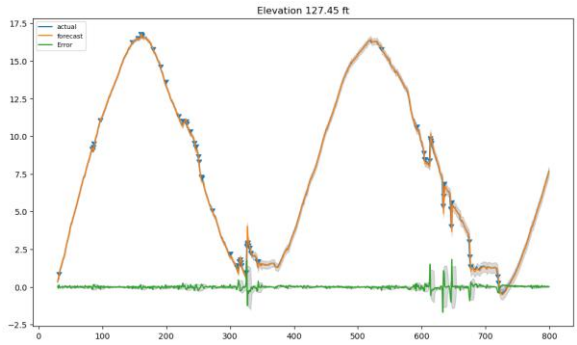

Figure 18) ARIMA prediction for the temperature time series at a 127.45 ft of elevation and its corresponding Forecast Error.

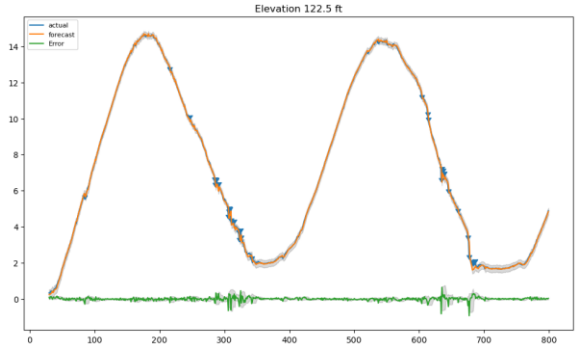

Figure 19) ARIMA prediction for the temperature time series at a 122.5 ft of elevation and its corresponding Forecast Error.

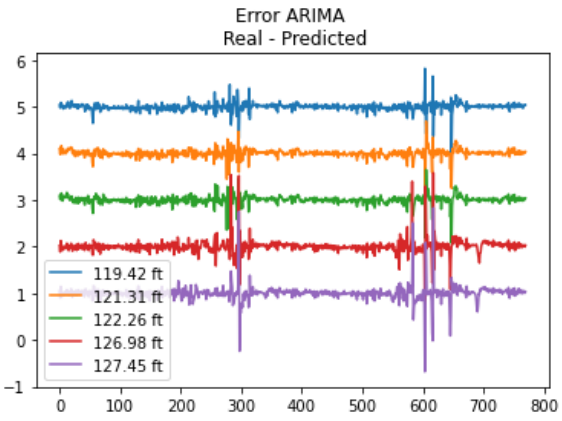

Figure 20) Forecast Errors in 5 different temperature time series.

4.2 PCA RESULTS

After selecting a threshold with a loss of 20 for the analysis with one principal component, the performance of the anomaly identification was of continuous detection of temperature anomalies. A continuous period between November 2016 and March 2017 was detected as anomalous, and a period between Jun and September of 2017 was detected as anomalous too. Small anomaly detections occurring in July 2017 was successful by not detecting the whole series of cold month as anomalous.

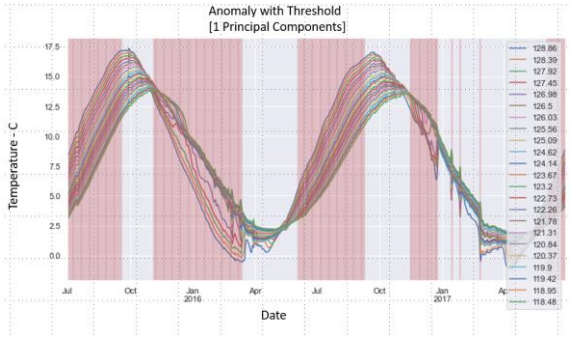

Figure 21) Temperature anomalies detected using 1 Principal Component.

There are more specific anomalies located between November 2016 and March 2017 using a threshold of a Loss with a value of 22, but more anomalous time zones where selected between October 2017 and June 2017 in comparison with the series reconstructed with one principal component.

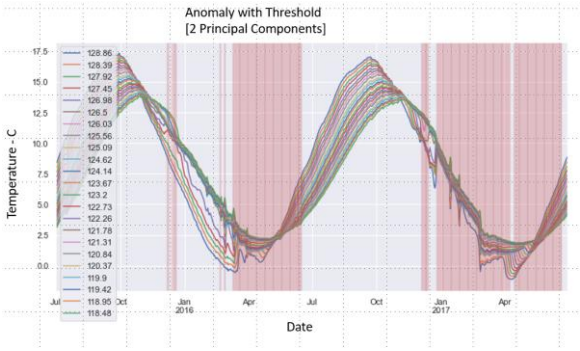

Figure 22) Temperature anomalies detected using 2 Principal Component2.

4.3 MULTIVARIATE DTW RESULTS

The two templates represented by heat maps are labeled as Anomaly_1 and Anomaly_2. Anomaly_1 is constructed by a heatmap constructed of 117 vs 35 elements. There are 6 breaks identified distributed along the series. The series of interest is composed by a heatmap with 8329 vs 35 elements. This represents a time zone between April 22nd 2015 and September 24th 2017 with an hourly average sampling rate.

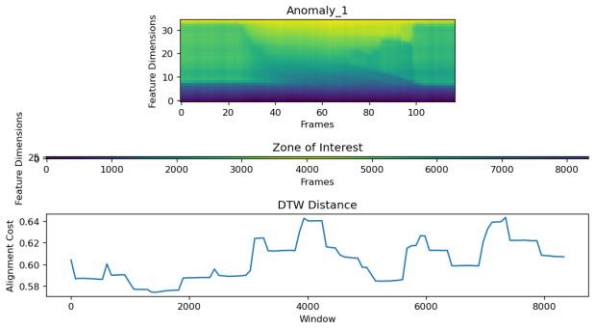

Figure 23) Multivariate DTW alignment cost for Temperature anomaly 1

The Anomaly_2 template is represented by a heatmap constructed by 3479 vs 35 array

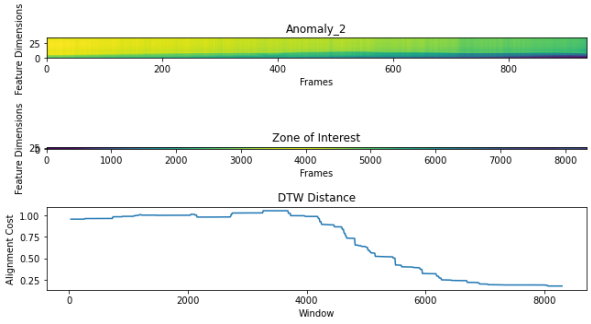

Figure 24) Multivariate DTW alignment cost for Temperature anomaly 2

4.4 GRANGER CAUSALITY RESULTS

After performing the evaluation of the 10 thermistors, it is found significance in 7 of them with a p-value less than .05

			p-value Causality
DTS -ele	**Thermistor**	**DTS/Thermistor**	**Grainger DTS/Thermistor**
124.62-ft	124.5 ft	No Multocolinearity	0.48
118.48-ft	118.06 ft	No Multocolinearity	0.14
111.87-ft	111.9 ft	No Multocolinearity	0.03
104.32-ft	104.19 ft	No Multocolinearity	0.00
82.61-ft	82.61 ft	No Multocolinearity	0.91
67.03-ft	67.2 ft	No Multocolinearity	0.00
50.98-ft	51.05 ft	No Multocolinearity	0.00
34.46-ft	34.64 ft	No Multocolinearity	0.00
18.42-ft	18.24 ft	No Multocolinearity	0.00

Figure 25) Granger Causality tests for DTS and thermistor string temperature.

			p-value Causality
DTS-ele	**Thermistor**	**DTS/Air**	**Grainger DTS/Air**
124.62-ft	124.5 ft	No Multocolinearity	0.71
118.48-ft	118.06 ft	No Multocolinearity	0.73
111.87-ft	111.9 ft	No Multocolinearity	0.76
104.32-ft	104.19 ft	No Multocolinearity	0.67
82.61-ft	82.61 ft	No Multocolinearity	0.03
67.03-ft	67.2 ft	No Multocolinearity	0.26
50.98-ft	51.05 ft	No Multocolinearity	0.83
34.46-ft	34.64 ft	No Multocolinearity	0.81
18.42-ft	18.24 ft	No Multocolinearity	0.91

Figure 26) Granger Causality tests for DTS and air temperature.

5. DISCUSSION

Performing ARIMA modeling for anomaly detection on the 5 time series selected, each series had different p,d,q order even when they look similar. From the Measuring Error obtained can be interpreted that there is a persistent series of anomalies in two time zones, corresponding to the cold months of the year, and that the magnitude of it is larger in the second period identified at higher elevations (127 and 126 ft), this can be interpreted that the anomaly grew in the second period of time and that the physical cause of it is greater in the higher elevation pseudo-nodes.

The PCA anomaly detection for time series detected all the major anomalous temperature events through the series with one principal component reconstructed, but other events that

are not considered anomalous occurring during the warm months were detected as anomalous by the loss calculation. Using a series with 2 principal components to calculate the loss and identify the errors had a better performance because it helps to localize most of the errors occurring in the cold months, and it didn't select the warm months as anomalous. The selection of the threshold from the loss for each analysis depends on the data owner expertise and it can be tuned based on it.

The Multivariate DTW worked well while identifying the thermal bag with a very low cost associated with it, with a difference of magnitude of 0.06. For the anomaly-1 template where visually are detected 7 events occurring in the same time lapse. It can be interpreted that there are 5 times identified with the template selected, but these events are propagated trough the whole series, when the original series the events are located only in the cold months of the year. The template for temperature anomaly 2 didn't perform well because the cost shape remained flat, and no visual pattern identification is detected.

Granger causality test indicate quite interesting results, the p-values obtained from the test shows that most of the elevations can from the thermistor temperature reading can provide useful information for predicting the DTS series at those specific locations. And the series with

For future work, it is necessary to complete the ARIMA analysis for the remaining elevation of the selected sones, to do an analysis of the error calculated from the real series and the predicted series. To identify where elevations present the larger errors and quantify their magnitude to interpret where the larger anomalies occur and when in time. For PCA analysis probably differentiating the series will help to identify mayor errors just as the ARIMA model and see the difference of calculating the loss between the real and the reconstructed series by using more principal components, with the aim of using the least amount of them. Multivariate DTW analysis can be tested to analysis other anomalies in the same time frame, and the same anomaly in other time lapses where there are continuous readings of the DTS. Now that Granger causality test gave some results depending on how the Air temperature and the temperature from the river may affect the forecasting of the DTS data, it would be ideal to extend this analysis with more data from the thermistor string.

6. REFERENCES

[1] Mactaquac Life Achievement Project. https://www.nbpower.com/en/about-us/projects/mactaquac-project. Mactaquac Life Achievement project. Accessed November 2, 2021

[2] Foster, M., Fell, R., & Spannagle, M. (2000). The statistics of embankment dam failures and accidents. *Canadian Geothecnical Journal*, 37(5), 1000-1024

[3] Shija, N.P., MacQuarrie, K.T.B., 2014. Numerical Simulation of Active Heat Injection and Anomalous Seepage near an Earth Dam-Concrete Interface. *International Journal of Geomechanics. (ASCE 2018),* **04014084**(1-11), doi: 10.1061(ASCE)GM.1943-5622.0000432

[4] Aufleger, M., Conrad, M., Goltz, M., Perzlmaier, S., & Porras, P. (2007). Innovative Dam Monitoring Tools Based on Distributed Temperature Measurement. Jordan Journal of Civil Engineering, 1(1), 29-37.

[5] Velásquez, J.P.P. (2007). Fibre optic temperature measurements: further development of the gradient method for leakage detection and localization in earthen structures. München: Technische Universität München.

[6] Aufleger, M., Goltz, M., Perzlmaier, S., & Dornstädter, J. (2008). Integral seepage monitoring on embankment dams by the DFOT Heat Pulse Method. Proceedings of the 1st International Conference on Long Time Effects and Seepage Behaviour of Dams.

[7] J. Zeng, L. Zhang, G. Shi, T. Liu and K. Lin, "An ARIMA Based Real-time Monitoring and Warning Algorithm for the Anomaly Detection," *2017 IEEE 23rd International Conference on Parallel and Distributed Systems (ICPADS)*, 2017, pp. 469-476, doi: 10.1109/ICPADS.2017.00068.

[8] E. H. M. Pena, M. V. O. de Assis and M. L. Proença, "Anomaly Detection Using Forecasting Methods ARIMA and HWDS," *2013 32nd International Conference of the Chilean Computer Science Society (SCCC)*, 2013, pp. 63-66, doi: 10.1109/SCCC.2013.18.

[9] A. H. Yaacob, I. K. T. Tan, S. F. Chien and H. K. Tan, "ARIMA Based Network Anomaly Detection," *2010 Second International Conference on Communication Software and Networks*, 2010, pp. 205-209, doi: 10.1109/ICCSN.2010.55.

[10] Y. Jin, C. Qiu, L. Sun, X. Peng and J. Zhou, "Anomaly detection in time series via robust PCA," *2017 2nd IEEE International Conference on Intelligent Transportation Engineering (ICITE)*, 2017, pp. 352-355, doi: 10.1109/ICITE.2017.8056937.

[11] D. Malioutov, "Beyond PCA for modeling financial time-series," *2013 IEEE Global Conference on Signal and Information Processing*, 2013, pp. 1140-1140, doi: 10.1109/GlobalSIP.2013.6737103.

[12] T. Tron, Y. S. Resheff, M. Bazhmin, D. Weinshall and A. Peled, "ARIMA-based motor anomaly detection in schizophrenia inpatients," *2018 IEEE EMBS International Conference on Biomedical & Health Informatics (BHI)*, 2018, pp. 430-433, doi: 10.1109/BHI.2018.8333460.

[13] D. Gaoming, X. Di, H. Wei, D. Zhantao and L. Wenlong, "Dynamic Time Warp Based Template Analysis," *2012 Second International Conference on Instrumentation, Measurement, Computer, Communication and Control*, 2012, pp. 470-473, doi: 10.1109/IMCCC.2012.116.

[14] J. Liang and Y. Zhou, "Clustering Multivariate Time Series from Large Sensor Networks," *2017 International Conference on Computer Systems, Electronics and Control (ICCSEC)*, 2017, pp. 563-567, doi: 10.1109/ICCSEC.2017.8447015.

[15] T. -T. -H. Phan, É. P. Caillault, A. Bigand and A. Lefebvre, "DTW-Approach for uncorrelated multivariate time series imputation," *2017 IEEE 27th International*

Workshop on Machine Learning for Signal Processing (MLSP), 2017, pp. 1-6, doi: 10.1109/MLSP.2017.8168165.

[16] S. Bhattacharjee and S. K. Ghosh, "Exploring spatial dependency of meteorological attributes for multivariate analysis: A granger causality test approach," *2015 Eighth International Conference on Advances in Pattern Recognition (ICAPR)*, 2015, pp. 1-6, doi: 10.1109/ICAPR.2015.7050660.

[17] M. Chvosteková, "A Measure of Prediction Precision for Granger Causality Analysis," *2021 13th International Conference on Measurement*, 2021, pp. 6-9, doi: 10.23919/Measurement52780.2021.9446790.

[18] Yang Yonghua, "China's technology progress and international trade: Granger causality test on China's data," *2012 International Conference on Information Management, Innovation Management and Industrial Engineering*, 2012, pp. 9-12, doi: 10.1109/ICIII.2012.6339907.